Copolymerization of Ethylene with Acrylonitrile Promoted by Novel Nonmetallocene Catalysts with Phenoxy-Imine Ligands

Xinli Zhang,[1] Zhi Liu,[1] Jianjun Yi,[2] Fengjiao Li,[1] Haibing Huang,[1] Wei Liu,[1] Hongpeng Zhen,[1] Qigu Huang,[1] Kejing Gao,[2] Wantai Yang[1]

[1]State Key Laboratory of Chemical Resource Engineering, Key Laboratory of Carbon Fiber and Functional Polymers, Ministry of Education, Beijing University of Chemical Technology, Beijing 100029, China
[2]Laboratory for Synthetic Resin Research Institution of Petrochemical Technology, China National Petroleum Corporation, Beijing 100083, China
Correspondence to: Q. Huang (E-mail: qgh96@yahoo.com.cn) or W. Yang (E-mail: huangqg@mail.buct.edu.cn)

Received 12 December 2011; accepted 1 February 2012; published online 23 February 2012
DOI: 10.1002/pola.25981

ABSTRACT: A series of novel nonmetallocene catalysts with phenoxy-imine ligands was synthesized by the treatment of phthaldialdehyde, substituted phenol with $TiCl_4$, $ZrCl_4$, and YCl_3 in THF. The structures and properties of the catalysts were characterized by ^1H NMR and elemental analysis. These catalysts were used for copolymerization of ethylene with acrylonitrile after activated by methylaluminoxane (MAO). The effects of copolymerization temperature, Al/M (M = Ti, Zr, and Y) ratio in mole, concentrations of catalyst and comonomer on the polymerization behaviors were investigated in detail. These results revealed that these catalysts were favorable for copolymerization of ethylene with acrylonitrile. Cat.**3** was the most favorable one for the copolymerization of ethylene with acrylonitrile, and the catalytic activity was up to 2.19×10^4 g PE/mol.Ti.h under the conditions: polymerization temperature of 50 °C, Al/Ti molar ratio of 300, catalyst concentration of 1.0×10^{-4} mol/L, and toluene as solvent. The resultant polymer was characterized by FTIR, cross-polarization magic angle spinning, ^{13}C NMR, WAXD, GPC, and DSC. The results confirmed that the obtained copolymer featured high-weight–average molecular weight, narrow molecular weight distribution about 1.61–1.95, and high-acrylonitrile incorporation up to 2.29 mol %. Melting temperature of the copolymer depended on the content of acrylonitrile incorporation within the copolymer chain. © 2012 Wiley Periodicals, Inc. J Polym Sci Part A: Polym Chem 50: 2068–2074, 2012

KEYWORDS: acrylonitrile; copolymer; ethylene; methylaluminoxane; nonmetallocene catalyst; structure

INTRODUCTION Traditional supported Ziegler–Natta catalyst and homogenous Ziegler–Natta catalysts such as metallocene catalyst and nonmetallocene catalyst are excellent for olefins (co-)polymerization.[1–4] However, it is challenging for the coordination copolymerization of ethylene with polar comonomer, because the nonbonded electron pair of the heteroatom from the polar comonomer tends to form complex with the center metal, resulting in that the transition metal catalyst is deactivated. So far, copolymers of ethylene with polar monomers mainly have been prepared by conventional radical process, which has poor stereo-controlling ability for polymers.[5] Thus, a preferred approach for the synthesis of functional polyolefins is the use of nonmetallocene catalyst, by changing the ligand structure of the catalyst to make the center metal less oxophilicit and to enhance the stereo-controlling ability for polymer. Fujita[6] reported highly selective formation of Al-PEs prepared by a bis(phenoxy-imine)Zr complex with methylalumoxane, which confirmed that the stereo-controlling ability of the nonmetallocene catalysts can be enhanced, and the molecular tailoring of polymer can be realized by changing ligand structure. Ye[7] prepared a series of new titanium complexes with two asymmetric bidentate β-enaminoketonato (N,O) ligands for ethylene polymerization. By changing the groups on benzene ring of the ligands, ethylene polymerization behavior was considerably influenced. Liu[8] synthesized a series of titanium complexes bearing phenoxy-phosphine or thiphenoxy-phosphine ligands, which efficiently promoted copolymerization of ethylene with methyl 10-undecenoate. In 2007, Nozaki[9] synthesized ethylene-rich linear copolymers of ethylene with acrylonitrile by isolated phosphine-sulfonate methylpalladium complex. It was observed for the first time that acrylonitrile units were inserted into a linear polyethylene chain. He found that acrylonitrile units were not only at the terminating end of the copolymer chain but also in the backbone. In 2009, Nozaki[10] reported copolymerization of ethylene with vinyl acetate promoted by Pd/alkylphosphine sulfonate catalyst, resulting in highly linear copolymers possessing in-chain and chain-end

© 2012 Wiley Periodicals, Inc.

VAc units. In 2010, Nozaki[11] continued to research the reason why incorporation of acrylonitrile to a linear polyethylene became possible using the phosphine-sulfonato Pd complex. He found that the P-SO_3 ligand facilitated both acrylonitrile insertion to alkyl Pd and ethylene insertion to α-cyanoalkyl Pd and that the β-hydride elimination was reasonably suppressed with P—SO_3. More important was that the experiment of ethylene/acrylonitrile copolymerization was realized by using the N—O/Pd complex with high-catalyst loading. This is a significant indication that the catalysts with N—O ligand highly promoting ethylene/acrylonitrile copolymerization would be possible. In 2010, Mecking[12] demonstrated that copolymerization of ethylene with acrylic acid was successful using neutral palladium(II) phosphine-sulfonato catalysts. Herein, we reported a kind of novel nonmetallocene catalysts bearing two phenoxy-imine groups that was used for copolymerization of ethylene with acrylonitrile with high-catalytic activity. The obtained copolymers featured narrow MWD, high-molecular weight (MW), and high-comonomer incorporation content. The effects of the ligand structures and the center metal atoms (Ti, Zr, and Y) of these catalysts and the polymerization conditions such as temperature, Al/M (M = Ti, Zr, and Y) ratio in mole and concentrations of catalyst and comonomer on the polymerization behaviors were investigated.

EXPERIMENTAL

General Remarks

All operations of air- and moisture-sensitive materials were performed using the rigorous repellency of oxygen and moisture in flamed Schlenk-type glassware on a dual manifold Schlenk line under nitrogen atmosphere. Phthaldialdehyde (99%) was purchased from J&K in China; 2-amino-4-methylphenol (98%) was purchased from TCI in China; 2-amino-5-methylphenol (98%) was purchased from Aldrich in China; 2-amino-4-*t*-butylphenol (97%) and methylaluminoxane (MAO) with 10 wt % in toluene were purchased from Acros Organics Agent in China. Toluene and THF from Beijing Chemicals Company were further purified by refluxing over sodium under normal pressures for 48 h prior use. Acrylonitrile was stored in a Schlenk tube containing 5 Å molecular sieves under high-purity nitrogen for 6 days prior use.

Characterization

^{1}H NMR spectra were recorded on a Varian INOVA600 MHz spectrometer in DMSO-d_6 solution at 25 °C, and tetramethyl silane (TMS) was used as reference. All ^{1}H chemical shifts were reported in parts per million relative to proton resonance in DMSO-d_6 at δ 2.62 ppm. Elemental analyses were performed on a Perkin–Elmer 2400 microanalyzer. FTIR spectra were recorded by a Nicolet 5DXC FTIR spectrograph. The spectra were obtained at a 40 cm^{-1} resolution, and average data were obtained from at least 32 scans in the standard wave number range from 500 to 4000 cm^{-1}. The instrument using for solid-state ^{13}C NMR was AV-300 system (Bruker) of 7.05 T and a multinuclear cross-polarization magic angle spinning (CP-MAS) probe. The diameter of zirconia rotor was 4 mm. The resonance frequency of ^{13}C was 75.432. Repetition delay for CP-MAS experiment was 10 s pulse sequence. The pulse width for excitation was 3.3 μs. The spectrum width of scanning was 350 ppm, and scanning times were 500–1000. The cross-polarization time of ^{13}C and ^{1}H was 3 ms. Typical spinning rate used for MAS and CP–MAS experiment was 5 kHz. The ^{13}C chemical shift was referenced to external TMS. The acrylonitrile incorporation content was estimated from CP-MAS ^{13}C NMR spectra. The average MW and molecular weight distribution (MWD) were measured by PL-GPC200 instrument using standard polyethylene as reference and 1,2,4-trichlorobenzene as solvent at 150 °C. DSC thermograms were recorded with a PA5000-DSC instrument at a rate of 10 K/min. WAXD curves were recorded with a Rigaku D/max 3A instrument, using Ni films to sieve wave, using Cu Kα radiation ($\lambda = 1.5405 \times 10^{-10}$ m). WAXD intensities were recorded from 5° to 40° with a continuous scanning speed.

Polymerization Procedure

All polymerization manipulations were carried out in a 300-mL reaction flask after purging all moisture and oxygen by a high-vacuum pump. Freshly distilled solvent (80 mL), desired amount of catalysts (Cat.**1–9**), and MAO were introduced in order. The mixture was stirred for 15 min for preactivation. Then injected desired amount of acrylonitrile using as comonomer, charged ethylene up to desired pressure, and heated the reactor to desired temperature. The system was stirred for 10 min. Finally, the reaction was terminated with 10 wt % HCl in alcohol. The obtained product was filtered, washed, then dried to constant weight in a vacuum oven at 80 °C, weighted it, and calculated the catalytic activity.

Synthesis of Catalyst Precursors

Phthaldialdehyde 0.68 g (5.0 mmol) and 2-amino-4-methylphenol 1.26 g (10.0 mmol) were dissolved in anhydrous alcohol of 50 mL. The mixture was refluxed for 8 h at 80 °C. Subsequently, the mixture was cooled to room temperature, and the precipitate was obtained. Then the precipitate was further purified by dissolved in anhydrous ether and recrystallized at −10 °C. About 1.48 g of **L1** with yield of 86.0% was obtained (Scheme 1), ^{1}H NMR (DMSO-d_6): δ 2.48 (s, 6H, methyl on benzene), δ 6.15–7.63 (m, 10H, benzene), δ 8.19 (s, 2H, C**H**=N), δ 8.97 (s, 2H, O**H**); **L1** ($C_{22}H_{20}N_2O_2$, F_W = 344), E_{LEM}. ANAL. Calcd: C, 76.81; H, 5.81; N, 8.14; found: C, 76.79; H, 5.83; N, 8.11. Ti complex of **L1** (Cat.**1**) was prepared by the treatment of **L1** 0.35 g (1.0 mmol) with $TiCl_4$ (0.11 mL, 1.0 mmol) in THF of 50 mL at 0 °C, adding Et_3N of 2.0 mmol. The reaction was lasted for 6 h at 40 °C. After filtrated, the solvent was removed, and the residue was dried by vacuum. Cat.**1** was obtained (0.39 g, 64.6%; Scheme 1). Cat.**1** was confirmed by ^{1}H NMR and microanalysis (Table 1). The ligand **L2** derived from 2-amino-5-methylphenol, **L3** from 2-amino-4-*t*-butylphenol, and Cat.**2–9** were synthesized according to the similar method mentioned earlier. Their ^{1}H NMR and microanalysis data were compiled in Table 1.

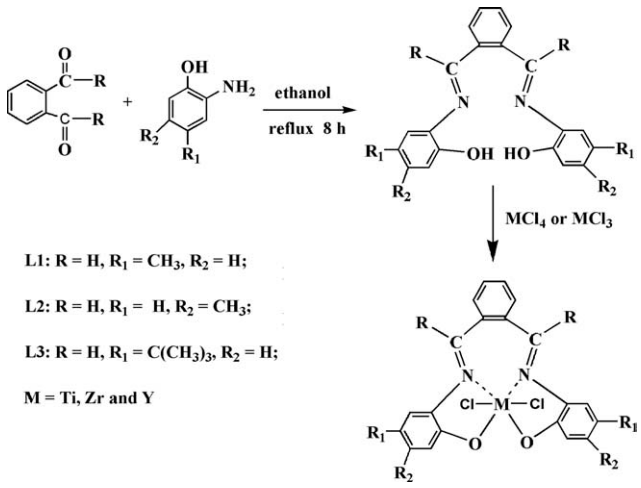

SCHEME 1 Synthesis of the nonmetallocene catalysts (the catalyst contains two chlorine atoms when M = Ti and Zr; while contains only one chlorine atom when M = Y).

RESULTS AND DISCUSSION

Copolymerization of Ethylene with Acrylonitrile

The novel nonmetallocene catalysts (Cat.**1–9**) were used for copolymerization of ethylene with acrylonitrile, using MAO as cocatalyst. The effects of the catalyst ligand structures and center metal atoms (Ti, Zr, and Y) on the copolymerization of ethylene with acrylonitrile were compiled in Table 2.

Compared to ethylene homopolymerization, the catalytic activity of copolymerization of ethylene with acrylonitrile was much lower. As expected, acrylonitrile was poisonous for the novel nonmetallocene catalysts system. However, a more electron-donating and higher steric hindrance ligand would be able to generate a less electrophilic metal center, which exhibited lower affinity ability to the polar functional group, giving rise to an enhanced catalytic activity. As showed in Table 2, different ligand structures of the complexes considerably influenced the copolymerization behavior of ethylene with acrylonitrile. The catalysts with L3 exhibited higher activity (runs 3, 6, and 9 in Table 2). For example, the catalytic activity of Cat.**3** was 1.77×10^4 g PE/mol.Ti.h (run 3 in Table 2), which was much higher than that of Cat.**1** and Cat.**2**. It might be ascribed to the bulk electron-donating group of tertiary butyl. The electron effectivity, caused by the ligand with tertiary butyl, resulted in an increase in electron density around Ti metal center, which reduced the ability for titanium to chelate with nitrogen atom from the comonomer, and thus the Ti complex can bear heteroatoms better. In addition, the steric effectivity of both the benzene ring around the active center, and the tertiary butyl could prevent the polar group (—CN) from chelating with metal centre.[13] Therefore, Cat.**3** exhibited the highest catalytic activity. And the MW of the obtained copolymer catalyzed by Cat.**3** was also higher.

From Table 2, it can be noticed that the center metal atom of these catalysts also had remarkable influences on the copolymerization of ethylene with acrylonitrile. Compared to Ti and Zr complexes (Cat.**1**–Cat.**6**), Y complexes (Cat.**7**–Cat.**9**) exhibited the lowest catalytic activity. Chemical bonds of most lanthanide complexes conventionally belong to electrovalent bonds with certain covalent characteristics.[13,14] This attributes to that 4f orbitals that play only a small role in forming the rare earth compound bonds, thus yttrium atom in the catalyst features strong oxophilicity. Apparently, it is much easier for yttrium atom to chelate with nitrogen atom from nitrile group (—CN) to form more steady complexes,[15] which led to a decrease in the catalytic activity of yttrium complexes. Compared to the Zr complexes, the Ti complexes

TABLE 1 The Parameters for Cat.1 to Cat.9

Catalysts	Metals	Ligands	Microanalysis	^{1}H NMR
Cat.**1**	Ti	L1	($C_{22}H_{18}N_2O_2TiCl_2$) (461): Calcd. C 57.32, H 3.90, N 6.08; Found C 57.29, H 3.91, N 6.11.	(DMSO): δ = 2.51 (s, 6H, methyl on benzene), 6.18–7.66 (m, 10H, benzene), and 8.22 (s, 2H, C**H**=N)
Cat.**2**	Ti	L2	$C_{22}H_{18}N_2O_2TiCl_2$) (461): Calcd. C 57.32, H 3.90, N 6.08; Found C 57.30, H 3.89, N 6.09.	(DMSO): δ = 2.53(s, 6H, methyl on benzene), 6.78–7.82 (m,10H, benzene), and 8.22 (s, 2H, C**H**=N)
Cat.**3**	Ti	L3	($C_{28}H_{30}N_2O_2TiCl_2$) (545): Calcd. C 62.85, H 5.94, N 4.89; Found C 62.87, H 4.88, N 4.90.	(DMSO): δ = 1.33 (s, 18H, *t*-butyl on benzene), 6.17–7.69 (m, 10H, benzene), and 8.20 (s, 2H, C**H**=N)
Cat.**4**	Zr	L1	$C_{22}H_{18}N_2O_2ZrCl_2$) (504): Calcd. C 52.39, H 3.57, N 5.55; Found C 52.41, H 3.56, N 5.57.	(DMSO): δ = 2.50 (s, 6H, methyl on benzene), 6.18–7.67 (m, 10H, benzene), and 8.21 (s, 2H, C**H**=N)
Cat.**5**	Zr	L2	$C_{22}H_{18}N_2O_2ZrCl_2$) (504): Calcd. C 52.39, H 3.57, N 5.55; Found C 52.40, H 3.58, N 5.54.	(DMSO): δ = 2.52(s,6H, methyl on benzene), 6.77–7.82 (m,10H, benzene), and 8.21(s, 2H, C**H**=N).
Cat.**6**	Zr	L3	($C_{28}H_{30}N_2O_2$ $ZrCl_2$) (588): Calcd. C 57.20, H 5.10, N 4.76; Found C 57.23, H 5.15, N 4.71.	(DMSO): δ = 1.32 (s, 18H, *t*-butyl on benzene), 6.16–7.69 (m, 10H, benzene), and 8.21 (s, 2H, C**H**=N)
Cat.**7**	Y	L1	($C_{22}H_{18}N_2O_2YCl$) (467): Calcd. C 56.58, H 3.85, N 6.00; Found C 56.49, H 3.87, N 6.02.	(DMSO): δ = 2.51(s,6H, methyl on benzene), 6.17–7.66 (m, 10H, benzene), and 8.21 (s, 2H, C**H**=N)
Cat.**8**	Y	L2	($C_{22}H_{18}N_2O_2YCl$) (467): Calcd. C 56.58, H 3.85, N 6.00; Found C 56.62, H 3.84, N 5.99.	(DMSO): δ = 2.54 (s, 6H, methyl on benzene), 6.77–7.83 (m, 10H, benzene), and 8.21 (s, 2H, C**H**=N).
Cat.**9**	Y	L3	($C_{28}H_{30}N_2O_2YCl$) (551): Calcd. C 61.03, H 5.44, N 5.08; Found C 61.05, H 5.49, N 5.11.	(DMSO): δ = 1.34 (s, 18H, *t*-butyl on benzene), 6.17–7.70 (m, 10H, benzene), and 8.22 (s, 2H, C**H**=N)

TABLE 2 Effects of the Metal Atoms and Structures of Catalyst Ligands on Copolymerization of Ethylene with Acrylonitrile

Run	Catalysts	A^a ($\times 10^{-4}$)	$M_w{}^b$ ($\times 10^{-4}$)	$M_w/M_n{}^b$	$T_m{}^c$ (°C)	Acry. Con^d (mol %)
1	Cat.**1** (Ti)	1.45	3.01	1.83	127.5	0.94
2	Cat.**2** (Ti)	1.28	3.35	1.80	127.6	0.93
3	Cat.**3** (Ti)	1.77	3.19	1.88	125.8	1.39
4	Cat.**4** (Zr)	0.76	2.02	1.79	123.9	2.18
5	Cat.**5** (Zr)	0.52	2.39	1.81	123.4	2.11
6	Cat.**6** (Zr)	0.95	1.85	1.84	122.5	2.26
7	Cat.**7** (Y)	Trace	–	–	–	–
8	Cat.**8** (Y)	0.17	0.92	1.77	108.7	2.28
9	Cat.**9** (Y)	0.38	1.05	1.82	112.5	2.25

[a] Catalytic activity, g P/mol.M.h.
[b] Determined by GPC.
[c] Determined by DSC.
[d] Acrylonitrile incorporation content, determined by ^{13}C NMR; polymerization conditions: concentration of catalyst, 1.0×10^{-4} mol/L; ethylene pressure, 0.2 MPa; acrylonitrile, 0.3 mol/L; temperature, 50 °C; n(Al)/n(M), 300; solvent, toluene, 80 mL; time, 10 min.

exhibited better ability to bear heteroatoms, and so the catalytic activity of the Ti complexes was higher for the copolymerization of ethylene with acrylonitrile.

The effects of polymerization conditions such as reaction temperature, Al/Ti ratio, and concentrations of catalyst and acrylonitrile on ethylene (co-)polymerization catalyzed by Cat.**3** were investigated. The results were listed in Table 3.

As shown in Table 3, with an increase of reaction temperature, the catalytic activity enhanced and reached the highest value of 1.77×10^4 gPE/molTi.h (run 3 in Table 3) at 50 °C and then decreased. It might attribute to that the temperature not only influences polymerization rate constant but also affects the concentration of monomer and stability of the activity center.[16] As seen in Table 3, with an increase of reaction temperature from 40 to 60 °C, the MW of obtained copolymers decreased gradually and MWDs became broader slightly. A possible explanation is that the weight–average MW of the obtained copolymers is determined by the ratio of $K_p/K_{tr.}$ With the increasing of the polymerization temperature, $K_{tr.}$ increases faster than $K_{p.}$ Therefore, rate of chain-transfer to monomer and MAO enhances much more than propagation reaction. However, acrylonitrile incorporation within copolymer chain changed slightly with varying temperature for Cat.**3**, which indicated that the reaction temperature was not an important factor to control the incorporation of acrylonitrile.

The Al/Ti molar ratio influenced the catalytic activity strongly. When the Al/Ti molar ratio ranged from 200 to

TABLE 3 Effects of Polymerization Conditions on Copolymerization of Ethylene with Acrylonitrile Catalyzed with Cat.3

Run	T^e (°C)	n(Al):n(Ti)	C^b ($\times 10^4$)	Acry^c (mol/L)	A^d ($\times 10^{-4}$)	$M_w{}^e$ ($\times 10^{-4}$)	$M_w/M_n{}^e$	$T_m{}^f$ (°C)	Acry. Con^g (mol %)
10	40	300	1.0	0.3	1.49	3.51	1.83	126.5	1.34
3	50	300	1.0	0.3	1.77	3.19	1.88	125.8	1.39
11	60	300	1.0	0.3	1.15	2.58	1.91	124.8	1.41
12	50	200	1.0	0.3	1.39	2.97	1.90	125.2	1.43
13	50	400	1.0	0.3	1.16	1.95	1.96	124.3	1.44
14	50	300	0.5	0.3	1.36	3.45	1.79	126.1	1.35
15	50	300	2.0	0.3	1.13	2.76	1.90	125.3	1.41
16	50	300	1.0	0	102	78.9	1.61	134.5	–
17	50	300	1.0	0.1	2.19	3.65	1.81	127.3	0.96
18	50	300	1.0	0.5	1.38	2.72	1.95	123.1	2.29

[a] Polymerization temperature.
[b] Concentration of catalyst (mol/L).
[c] Charged acrylonitrile concentration (mol/L).
[d] Catalytic activity (g P/mol.Ti.h).
[e] Determined by GPC.
[f] Determined by DSC.
[g] Acrylonitrile incorporation content, determined by ^{13}C NMR; polymerization conditions: ethylene pressure, 0.2 MPa; solvent, toluene, 80 mL; time, 10 min.

300 (runs 12 and 3 in Table 3), the catalytic activity increased and reached the maximum value of 1.77×10^4 gPE/molTi.h at n(Al):n(Ti) = 300 (run 3 in Table 3). The catalytic activity decreased with further increasing the Al/Ti molar ratio. The addition of MAO influenced the MWs and MWDs of the obtained polymers. MAO as a cocatalyst acts as a catalyst precursor for alkylation, a chain-transfer agent, and a deimpurifier. Trimethylaluminum in MAO can reduce oxidation state of Ti (IV) to Ti (III), while Ti (IV) is favorable for α-olefin polymerization.[17] When the amount of MAO is smaller, part of active center is transferred to β-H, resulting in lower activity, lower MWs, and broader MWDs. Although when excess MAO is introduced, it might be easier for the propagating chain transferring to MAO, resulting in lower MWs and broader MWDs of the obtained polymers. So only when the amount of MAO is proper, can the active center be stable and chain transfer to β-H and MAO be controlled effectively. Moreover, acrylonitrile incorporation within the copolymers had minor changes with varying Al/Ti molar ratio, which implied that the comonomer incorporation did not mainly depend on the Al/Ti molar ratio.

The catalytic activity for copolymerization of ethylene with acrylonitrile exhibited the highest value of 1.77×10^4 g PE/molTi.h under the catalyst concentration of 1.0×10^{-4} mol/L. When the catalyst concentration changed from 0.5×10^{-4} to 1.0×10^{-4} mol/L (runs 14 and 3 in Table 3), the catalytic activity increased from 1.36×10^4 to 1.77×10^4 g P/mol.Ti.h. But when the catalyst concentration further increased to 2.0×10^{-4} mol/L (run 15 in Table 3), the catalytic activity decreased to 1.13×10^4 g P/mol.Ti.h. It may attribute to that when the catalyst concentration is lower than 1.0×10^{-4} mol/L, the number of activity species was smaller. Maybe a higher fraction of the activity species was poisoned by impurity in the solution and inside the syringe. But if the catalyst concentration was higher than 1.0×10^{-4} mol/L, the polymerization process became faster, which would lead to greater amounts of polymer produced by the same-scale manipulation at the same time. Therefore, the polymer chain could be entangled easier, giving rise to decline in the overall chain propagation rate. In addition, the catalyst concentration influenced the insertion content of acrylonitrile slightly, implying that the comonomer incorporation was not mainly depended on the concentration of the catalyst either.

As shown in Table 3, the activity of cat.**3** toward the copolymerization and comonomer incorporation was considerably influenced by the comonomer feed ratios. With an increase in the quantity of the acrylonitrile charged from 0.1, 0.3, to 0.5 m/L, the acrylonitrile contents of the copolymers enhanced from 0.96, 1.39, to 2.29 mol %, respectively. But the catalytic activity sharply decreased from 2.19×10^4, 1.77×10^4, to 1.38×10^4 g P/mol.Ti.h (runs 17, 3, and 18 in Table 3). Whereas the catalytic activity for ethylene homopolymerization was 1.02×10^6 g P/mol.Ti.h (run 16 in Table 3). The decline of catalytic activity might be ascribed to both the low-insertion rate of the polar monomer and the last-inserted functional α-olefin suppressing ethylene coordination and insertion. Similarly, the MWs of the resultant copolymers also decreased from 3.65×10^4, 3.19×10^4, to 2.72×10^4 g/mol upon increasing acrylonitrile concentration in feed from 0.1, 0.3, to 0.5 m/L, respectively (runs 17, 3, and 18 in Table 3) due to low rate of propagation reaction, comparison with the chain transfer.[18] The MWDs of the resultant polymers almost kept about 2, indicating that the single-site catalyst system was confirmed.

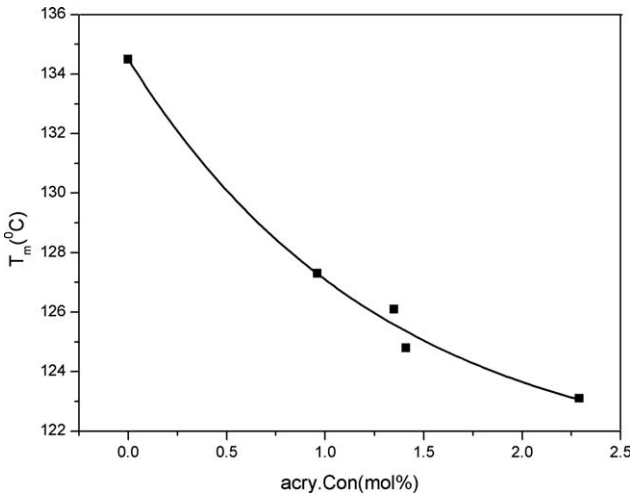

FIGURE 1 Variation of melting temperature of polymers versus acrylonitrile incorporation.

From Table 2, we can note that the melting temperatures of the resultant polymers decreased with the decline of MWs, but increased with the decline of the acrylonitrile contents in the copolymers. For example, the two copolymers (runs 6 and 9 in Table 2) showed different melting temperatures, 122.5 °C for run 6 and 112.5 °C for run 9. Even though their acrylonitrile incorporation contents were almost the same, 2.26 mol % for run 6 and 2.25 mol % for run 9, they had different MWs, 1.85×10^4 g/mol for run 6 and 1.05×10^4 g/mol for run 9. As shown in Figure 1 (the data from Table 3), DSC results showed that the melting temperatures of the resultant polymers gradually decreased with increasing the acrylonitrile contents of the copolymers, and only one melting temperature was observed, implying that the resultant copolymer possessed uniform acrylonitrile incorporation.[18] These results indicated that the melting temperatures of the copolymers were influenced by MWs and acrylonitrile incorporation contents.

Characterization of the Polymer

The CP-MAS ^{13}C NMR spectrum of the polyethylene promoted by Cat.**3** (run 16 in Table 3) was carried out [Fig. 2(a)]. Only methylene peaks were recognizable in the spectra. The peaks at δ 33.7, 32.3, and 31.3 ppm were assigned to methylene carbons from monoclinic crystalline, orthorhombic crystalline, and amorphous fraction, respectively.[19] Any other signals were not shown, which confirmed that the obtained polymer was linear polyethylene without branch. The CP-MAS ^{13}C NMR spectrum of the copolymer of ethylene with acrylonitrile (run 18 in Table 3) was presented in Figure 2(b). The weak signal at δ 14–15 ppm exhibited the

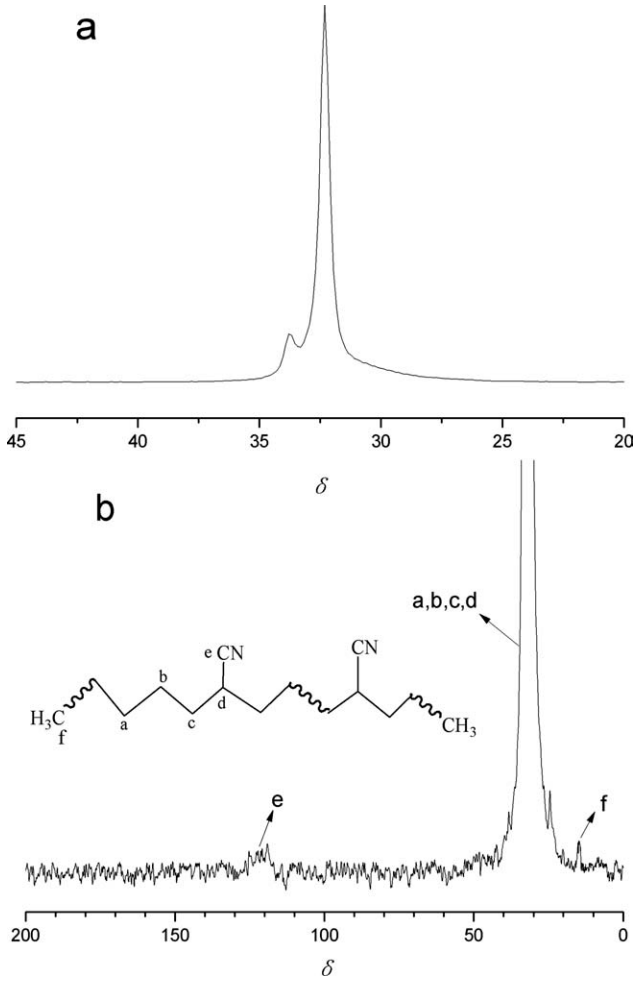

FIGURE 2 CP-MAS ^{13}C NMR spectra of (a) polyethylene from run 16 in Table 3 and (b) ethylene/acrylonitrile copolymer from run 18 in Table 3.

existence of —CH_3, which was located at the end of the copolymer chain. The signals at 20–40 ppm represented methylene and methine of the copolymer backbone and that at 115–125 ppm represented the side group of —CN. The result confirmed that acrylonitrile was inserted into the copolymer chain indeed. The area integral ratio of the resonance peaks of methylene, methane (δ = 20–40 ppm) to nitrile group (δ = 115–125 ppm) was 87.5:1. That was to say x/y = (87.5–2)/2 = 85.5/2 = 42.75/1. So, the content of acrylonitrile that was inserted into copolymer was $y/(x + y) = 1/(42.75 + 1) = 2.29$ mol %, Where x was defined as the number of ethylene units and y defined as the number of acrylonitrile units within the copolymer chain.

There are two main patterns of chain transfer in the copolymerization process catalyzed by nonmetallocene catalyst. One is that β-H transfers to active center and monomer; the other is that the growing chain transfers to MAO. The former obtains polymer with unsaturated end group, while the latter obtains polymer with saturated end group. Chain termination reaction of olefin polymerization catalyzed by nonmetallocene catalyst can also get polymer with saturated end group. From Figure 2(b), we can see that there was no signal that represented the unsaturated carbon–carbon double bond, but a signal at δ 14–15 ppm assigned to methyl was observed, implying that the obtained copolymer of ethylene with acrylonitrile, catalyzed by the catalyst system of Cat.**3**/MAO, was featured with methyl group at the chain end. The result confirmed that the dominant chain transfer was chain transfer to MAO.

According to Figure 2(b), the area integral ratio of the resonance peaks of methylene and methane (δ = 20–40 ppm) to methyl group (δ = 14–15 ppm) was ~486, which implied that the copolymer molecular chain was comprised of 475 vinyl units and 11 acrylonitrile units. The number of acrylonitrile units was calculated by the content of acrylonitrile inserted into copolymer mentioned earlier. The vinyl unit of 475 was given by (486–11). Therefore, the number–average MW (M_n) of the copolymer was calculated by the equation: $M_n = 475 \times 28 + 11 \times 53 = 13{,}900$ g/mol (28 is the MW of ethylene, 53 is the MW of acrylonitrile), which was in keeping with the result of GPC.

The FTIR plots of the obtained polymers were performed (Fig. 3). The wave numbers at 2918, 2850, 1471, and 719 cm^{-1} were characteristic of linear polyethylene. We can see from the FTIR spectrums of the copolymers in Figure 3, except for all the signals as same as polyethylene, there was another signal near 2243 cm^{-1} representing —CN group within the copolymers of b, c, and d. The signal at 719 cm^{-1} represented the long chain units [$(CH_2)_n$, $n \geq 4$] of polyethylene, but there was no signal at 719 cm^{-1} for polyacrylonitrile [Fig. 3(e)]. So, we can obtain the fraction of acrylonitrile inserted into the copolymer chain by the ratio of integral area of the absorption peak at 2243 cm^{-1} to that at 719

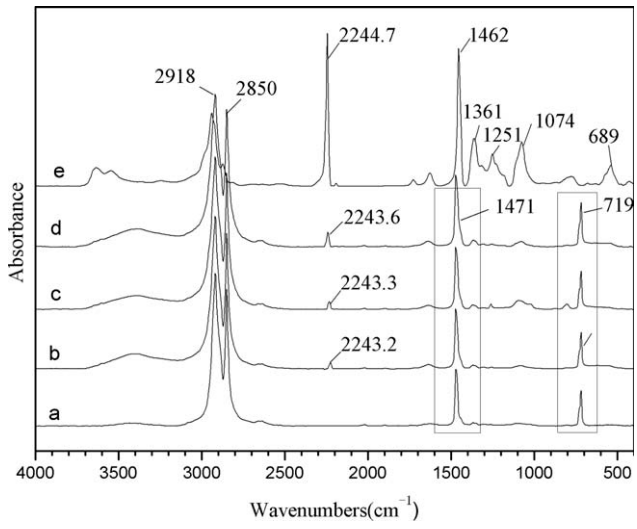

FIGURE 3 FTIR spectrums of ethylene homopolymer (a, run 16 in Table 3) and ethylene/acrylonitrile copolymer (b, run 3 in Table 3; c, run 17 in Table 3; d, run 18 in Table 3) and polyacrylonitrile (e, obtained by radical polymerization, AIBN used as initiator at 65 °C for 4 h).

cm^{-1} [Fig. 3(b–d)]. As for the copolymer d [Fig. 3(d)], the ratio of A_{2243}/A_{719} was 0.335, where A_{2243} was defined as the integral area of the absorption peak at 2243 cm^{-1} and A_{719} was defined as the integral area of the absorption peak at 719 cm^{-1}. And we have calculated the acrylonitrile incorporation for the copolymer d was 2.29 mol %. For the copolymers b and c [Fig. 3(b,c)], the ratios of A_{2243}/A_{719} were 0.141 and 0.204, respectively. The acrylonitrile incorporation of the copolymer d was used as reference; thus, the acrylonitrile contents of the copolymer b and c were 0.96 and 1.39 mol %, respectively. Compared to polyacrylonitrile, the signals of —CN side group of the copolymers b, c, and d moved toward blue area and became 2243.2, 2243.3, and 2243.6 cm^{-1} (Fig. 3), respectively. The result revealed that the wave number of —CN side group of the copolymer increased with increasing the acrylonitrile incorporation content within the copolymer chain.

CONCLUSIONS

The novel nonmetallocene catalysts consisting of phenoxyimine ligands, Cat.**1**–Cat.**9**, exhibited high-catalytic activity for the copolymerization of ethylene with acrylonitrile. Under the typical polymerization condition: temperature of 50 °C, Al/Ti molar ratio of 300, concentration of catalyst with 1.0×10^{-4} mol/L, toluene as solvent, and the catalytic activity of the copolymerization of ethylene with acrylonitrile was of up to 2.19×10^4 g PE/molTi.h. Both the results of FTIR and solid ^{13}C NMR indicated that the structure of the obtained polyethylene was linear and the copolymer of ethylene with acrylonitrile catalyzed by Cat.**3** had the highest acrylonitrile incorporation content up to 2.29 mol %. Acrylonitrile units within the copolymer chain were isolated by ethylene units. Block distribution of ethylene units was dominant in the copolymer chain. The GPC results confirmed that the obtained polymers featured higher MW up to 3.65×10^4 g/mol and narrow M_w/M_n ratio within 2.

Financial support for this work from the National Natural Science Foundation of China (Grant No. 21174011), the Natural Science Foundation of Beijing, China (Grant No. 2102036), and Major Project for Polymer Chemistry, Physics Subject Construction from Beijing Municipal Education Commission (BNEC) (XK100100540, XK100100640).

REFERENCES AND NOTES

1 Bialk, M.; Czaja, K. *Polymer* **2000,** *41*, 7899–7904.

2 Kong, Y.; Yi, J. J.; Dou, X. L.; Liu, W. J.; Huang, Q. G.; Gao, K. J.; Yang, W. T. *Polymer* **2010,** *51*, 3859–3866.

3 Luo, H. K.; Tang, R. G.; Gao, K. J. J. *Catal.* **2002,** *210*, 328–339.

4 Huang, Q. G.; Sheng, Y. P.; Yang, W. T. J. *Appl. Polym. Sci.* **2007,** *103*, 501–505.

5 Ittel, S. D.; Johnson, L. K.; Brookhart, M. *Chem. Rev.* **2000,** *100*, 1169–1204.

6 Saito, J.; Tohi, Y.; Matsukawa, N.; Mitani, M.; Fujita, T. *Macromolecules* **2005,** *38*, 4955–4957.

7 Ye, W. P.; Zhan, J.; Pan, L.; Hu, N. H.; Li, S. Y. *Organometallics* **2008,** *27*, 3642–3653.

8 He, L. P.; Hong, M.; Li, B. X.; Liu, J. Y.; Li, Y, S. *Polymer* **2010,** *51*, 4336–4339.

9 Kochi, T.; Noda, S.; Yoshimura, K.; Nozaki, K. J. *Am. Chem. Soc.* **2007,** *129*, 8948–8949.

10 Ito, S.; Munakata, K.; Nakamura, A.; Nozaki, K. J. *Am. Chem. Soc.* **2009,** *131*, 14606–14607.

11 Nozaki, K.; Kusumoto, S.; Noda, S.; Kochi, T.; Chung, L. W.; Morokuma, K. J. *Am. Chem. Soc.* **2010,** *132*, 16030–16042.

12 Runzi, T.; Frohlich, D.; Mecking, S. J. *Am. Chem. Soc.* **2010,** *132*, 16623–16630.

13 Maron, L.; Eisenstein, O. J. *Phys. Chem. A* **2000,** *104*, 7140–7143.

14 Vicentini, G.; Zinner, L. B.; Aricóa, E. M.; Zinnera, K.; Matosa, J. R.; De Matos, J. E. X. *Thermochim. Acta* **1993,** *228*, 137–146.

15 Terao, H.; Ishii, S.; Mitani, M.; Tanaka, H.; Fujita, T. J. *Am. Chem. Soc.* **2008,** *130*, 17636–17637.

16 Ma, L.; Wang, H. L.; Yi, J. J.; Huang, Q. G.; Gao, K. J.; Yang, W. T. J. *Polym. Sci., Part A: Polym. Chem.* **2010,** *48*, 417–424.

17 Huang, Q. G.; Wu, Q.; Zhu, F. M.; Lin, S. A. J. *Polym. Sci., Part A: Polym. Chem.* **2001,** *39*, 4068–4074.

18 Mu, J. S.; Liu, J. Y.; Liu, S. R.; Li, Y. S. *Polymer* **2009,** *50*, 5059–5064.

19 Hana, O. H.; Chaea, S. A.; Hanb, S. O.; Woob, S. K. *Polymer* **1999,** *40*, 6329–6336.